INTERACTION OF LASER-INDUCED STRESS WAVES WITH METALS

A. H. Clauer
B. P. Fairand

BATTELLE
Columbus Laboratories
505 King Avenue
Columbus, Ohio 43201

ABSTRACT

The effect of high intensity laser induced stress waves on the hardness and tensile strength of 2024 and 7075 aluminum and on the fatigue properties of 7075 aluminum were investigated. Laser shocking of these alloys increases the hardness of the underaged 2024-T351 but has little or no effect on the peak aged 2024-T851 and 7075-T651 or the over-aged 7075-T73. The largest increases in tensile strength were observed in 7075-T73, lesser increases in 2024-T351 and none in 2024-T851 or 7075-T651. The fretting fatigue life of fastener joints of 7075-T6 was increased by orders of magnitude by laser shocking the region around the fastener hole before drilling and assembling. Also the fatigue crack propagation rates were significantly decreased by laser shocking.

INTRODUCTION

The effects of high amplitude stress waves on the micro-structure and properties of metals and alloys have been the subject of numerous investigations. These stress waves are often generated by explosive charges or impact between a projectile and the target specimen. One of the interesting effects is that the shock waves can develop significant plastic strains in the metal with a smaller equivalent change in the specimen dimensions than required by more conventional metal working processes. This led to investigations of the effects of shock treatments on strength and hardness, fracture toughness, stress corrosion cracking, thermomechanical processing, and other properties (1-4). While in some of these areas the benefit derived from shock deformation

compared to conventional working is not always clear, it is established that shock waves can produce high dislocation densities with attendant effects on material properties. However, systems design considerations associated with handling explosives or using driver plates for materials processing make application of shock processing difficult.

Another source of high intensity stress waves is the high energy pulsed laser. This potential was first recognized and explored in the early nineteen sixties (5,6). Subsequent work established the conditions for major enhancement of the amplitude of the stress waves, making it possible to plastically deform metals when irradiating in air at standard conditions (7-11). This stimulated interest in using these laser induced pressure waves to alter the properties of materials in a manner similar to high explosive and flyer plate shock deformation of metals and alloys.

This paper presents the results of investigations on the effects of laser induced stress waves on the hardness, tensile strength, and fatigue life of several aluminum alloys. Although some of the results are from a limited number of experiments, they are of sufficient interest in showing the potential of laser shock processing that they are presented here.

LASER INDUCED STRESS WAVES

The mechanism for the development of the stress waves has been presented in detail in a recent paper, but a brief description will be given here (12). When the intense laser beam strikes the metal surface, the surface layer is instantaneously vaporized. The rapidly expanding high temperature vapor exerts a pressure on the target surface which then propagates into the specimen as a stress wave. Higher surface pressures are obtained by placing on the target surface an overlay transparent to the laser beam, such as fused quartz or water, which confines the 'blow-off' material between it and the specimen surface for the duration of the laser pulse. The rapid thermal expansion of this confined vapor produces the enhanced peak pressures necessary for plastic deformation of the target specimen.

The specimen surface can be protected and peak pressures further modified by applying an opaque overlay between the transparent overlay and the specimen surface. Black paint serves to protect the surface with no loss in peak pressure and is easily removed after the laser irradiation (10,12). Metallic overlays such as lead and zinc, having different sublimation and ionization energies, and thermal conductivities can be used to tailor the shape and amplitude of the stress waves (12,13). In addition to the surface overlays, the peak pressure can be controlled by changing the power density of the laser beam. Over a range of power densities and for many of the surface conditions studied, the peak pressure is proportional to the square root of peak power density (12).

Typical stress wave profiles are shown in Figure 1. The shape of these waves is similar to the shape of the laser pulse intensity. The rise time is similar for both, but the tail on the stress wave is longer lasting than the laser pulse because the decay time of the stress wave is influenced

by the thermal behavior of the trapped blow-off vapor. Using appropriate surface overlays and laser beam parameters, peak surface pressures of 10 GPa or more are possible.

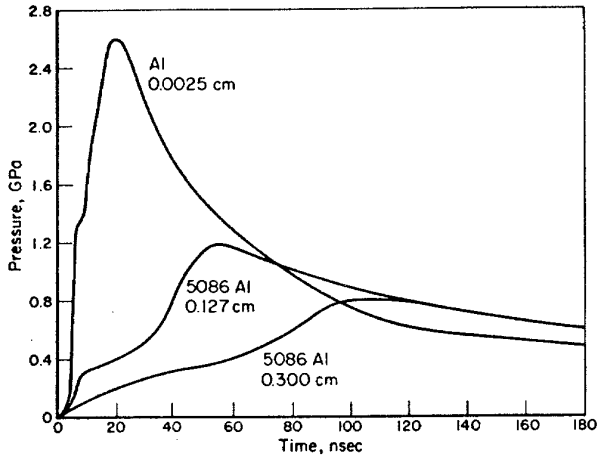

Fig. 1. Pressure Wave Profiles Measured at the Back Surface of Aluminum Specimens Having the Thicknesses Indicated by Each Curve.

EXPERIMENTAL CONDITIONS

Laser Conditions

The laser system is a high power CGE VD-640 neodymium glass laser consisting of a Q-switched laser oscillator followed by six amplifier stages. The laser pulse which was used in most of the experiments is triangular in shape with a pulse length having a full width at half maximum of 20 to 30 nsec. Laser spot diameters varied from 0.6 to 3 cm. The surface conditions usually consisted of a black paint overlay covered by a transparent overlay of fused quartz or water.

The specimens were irradiated under several different experimental configurations. The simplest was irradiation from one side with the back side either unsupported or backed up against an aluminum back-up block. Most of the radiations were made on two sides simultaneously by splitting the laser beam and steering each half to strike the opposite sides of the specimen simultaneously. This has certain advantages which will be discussed later.

Materials

The aluminum alloys were received as 6.4 mm thick plate of 2024-T351 and 7075-T651. The 2024-T851 was obtained by aging the 2024-T351 material 10 hours at 190° C and air cooling. The material had the expected microstructure consisting of pancake-shaped grains containing a dislocation sub-structure and an intermediate precipitate probably composed of Mn-rich aluminum compounds. The aging treatment used to reach the T851 condition coarsens the grain size somewhat and produces a fine precipitate of lathe-shaped S phase. The 7075-T73 temper was

obtained by solution treating the 7075-T651 for 1 hour at 465° C and cold water quenching followed by a two step aging sequence: 7 hours at 110° C plus 15 hours at 175° C. The microstructure of the as-received peak-aged T651 condition consisted of pancake-shaped grains containing a chromium-rich intermediate precipitate, a fine precipitate of G.P. zones, and a small amount of η' (a partially coherent precipitate which ages to form $\eta(MgZn_2)$). Overaging the 7075 aluminum to the T73 condition coarsened the grain size and produced a precipitate of η' and η.

SHOCK HARDENING AND STRENGTHENING

As part of the investigation of the surface and in-depth effects of laser shock hardening, the surface and subsurface hardness and the tensile properties of the alloys were determined before and after laser shocking. In many cases the surface hardness was measured on the tensile specimens before tensile testing. Most experiments were made on specimens 0.1 cm thick having 0.01 to 0.03 cm ground off each surface with No. 600 paper to remove the work hardened machining layer. Some experiments were conducted on 0.3 cm thick specimens. The gage length of the flat tensile specimens was 0.5 cm wide by 1.5 cm long. Black paint and fused quartz overlays were used for most of the shots, but black paint plus water overlays were used for a few.

2024 Aluminum. The effect on surface hardness from increasing the amplitude of the laser induced stress wave depended on the temper of the alloy. The peak pressure was increased by increasing the power density of the laser beam. The surface hardness of the underaged 2024-T351 increased with increasing peak pressure as shown in Figure 2a, whereas the aged 2024-T851 showed no hardness increase over the same range, Figure 2b. Surface hardness for specimens irradiated on one side and for specimens irradiated on both sides simultaneously are included in the Figures. The peak pressures were obtained from the values of peak power density monitored during the experiment and the relation between peak power density and peak pressure (12).

A perspective of the laser shocking results can be had by comparing them with results obtained by shocking similar material with a flyer plate. Herring and Olson shocked 2024 aluminum in similar heat treated conditions to those studied here*, with a thin mylar flyer plate,

---

*Their underaged condition was solution treated (ST) and aged 1 hour at 190° C. The T351 condition was ST then cold stretched 1.5 to 3%. The initial hardness of these two conditions is similar (square at zero pressure in Figure 2a). Their peak aged, T6, condition was ST and aged 12 hours at 190° C compared to the T851 condition obtained by aging the T351 material 10 hours at 190° C. The initial hardness of these two conditions is also similar (Figure 2b).

producing a range of shock pressures of 150 nsec duration (14). These data are included as the open squares in Figure 2. For 2024-T351, there is a trend for the laser shocking results to define a rapid shock hardening region with increasing peak pressure at pressures below 5 GPa. The flyer plate results are consistent with this rapid hardening and also show a saturation of shock hardening

above 5 GPa. This saturation hardness is the same as the hardness of a heavily hammered surface, 165 to 178 DPH. The suggestion of a lower saturation hardness by the laser shocking points above 5 GPa might be due to the short pulse duration of the higher pressure shots compared to the flyer plate pulse duration. It has been shown that hardening effects can increase with increasing duration of the shock wave for a constant pressure amplitude (15,16).

The lack of shock hardening of 2024-T851 is also consistent with the flyer plate results (Figure 2b). The laser shocking pressures were all below the threshold pressure for surface hardening of 8 to 10 GPa indicated by the flyer plate data. However, this pressure threshold is within the upper pressure range attainable with the pulsed laser.

The hardness profile across the laser irradiated region is relatively uniform, Figure 3. This is desirable if a shocked area larger than a single spot is required for a particular application of laser shock processing, in that it decreases the amount of overlap of neighboring spots necessary for complete area coverage.

The depth of the hardening below the surface is limited by the short duration and triangular shape of the stress wave. The peak pressure of the shock wave decreases rapidly both because the trailing rarefaction wave rapidly overtakes the shock front and from the work used to plastically strain the metal. The rapid decrease in peak pressure can be seen in Figure 1. Because of this decrease in pressure, the shock hardening effect decreases rapidly from a maximum at the shocked surface to zero within 1 to 2 mm below the surface. To obtain more uniform in-depth hardening to increase yield strength, for example, the specimen is shocked from both sides simultaneously. This not only hardens the opposite surfaces but also hardens the center of the specimen where the shock waves traveling from the opposing surfaces momentarily add and double the local peak pressure. The through-thickness hardness profile is shown in Figure 4 for a 0.09 cm thick specimen. Similar effects were observed in a 0.3 cm thick specimen (17).

The influence of laser shocking on the tensile strength of these alloys is modest for the peak pressure range investigated. The 2024-T351 condition had a maximum of 6 percent increase in yield strength* and a few percent increase in ultimate strength at a peak pressure of 3.4 GPa, whereas the surface hardness increased over 15 percent. The 2024-T851 showed no

---

*The unshocked tensile properties for the two conditions were 351 MPa 0.2 percent offset yield strength and 473 MPa ultimate strength for 2024-T351 and 445 MPa 0.2 percent offset yield strength and 483 MPa ultimate strength for 2024-T851 (17).

increase in tensile strength after laser shocking. For each alloy the total elongation decreased after laser shocking as is often observed in strain hardened metals, but the reduction in area often increased (17).

Earlier work on laser shocking welded 5054 and 6061 aluminum showed increases in the yield strength of the weld and heat affected zones of 50 percent after laser shocking compared to the welded condition (19). Greater strengthening may be possible with higher pulse durations and peak pressures. Otto performed flyer plate experiments on 2024 aluminum in a condition similar to 2024-T351 using a 1000 nsec pulse duration (18). The longer pulse duration would be expected to combine more uniform through thickness hardening and possibly higher strengths at the same peak pressure compared to the shorter laser induced shock waves (15,16). At about 6 GPa and above, Otto reported increases of over 40 percent at the yield strength of his 2024-T3 material (18).

The shock hardening and strengthening observed in these alloys must originate from the dislocation substructure produced in the specimen by the shock waves. The microstructures after laser shocking were studied in thin foils by electron transmission microscopy. The foils were taken from the mid-thickness of 0.3 cm thick discs laser shocked from both sides. The microstructures near the surfaces are expected to have higher dislocation densities because the post-shock hardness and plastic strain is higher near the surface.

The microstructures before and after shocking are shown in Figure 5. In 2024-T351 the dislocations are arranged in a uniform distribution of tangles in agreement with shocked substructures observed in two similar Al-Cu-Mg alloys at the same peak pressure and in 2024-T3 shocked at 6.5 GPa (20,18). With the Al-Cu-Mg alloys, cold rolling to 4 percent strain would produce a somewhat coarser, but still relatively uniform substructure (20). This differs from the behavior of pure aluminum, which shows a dislocation cell structure after cold rolling, but after shocking may show either a uniform distribution of dislocation tangles, contrary to what is expected on the basis of a high stacking fault metal, or a cellular dislocation substructure (20-22). The microstructure of 2024-T851 after shocking at a lower peak pressure than the 2024-T351 also contains a relatively uniform distribution of dislocations (Figure 5d). A similar result, but with an apparently high dislocation density after shocking, was reported for 2024-T6 (14).

One of the reasons for the different shock hardening response of the T351 and T851 conditions can be found in the difference in their strain hardening behavior. The T351 condition strain hardens much more than the T851 condition. The difference between the tensile yield strength and ultimate strength gives a crude comparison of the strain hardening rates between the two conditions. The ultimate tensile strengths of the two conditions are similar, 473 and 483 MPa, whereas the yield strengths are 357 and 445 MPa for the T351 and T851 conditions, respectively. Thus, not only are higher pressures required to cause yielding in 2024-T851, but more important, equivalent plastic strains will increase the flow stress of 2024-T351 more than it will that of 2024-T851.

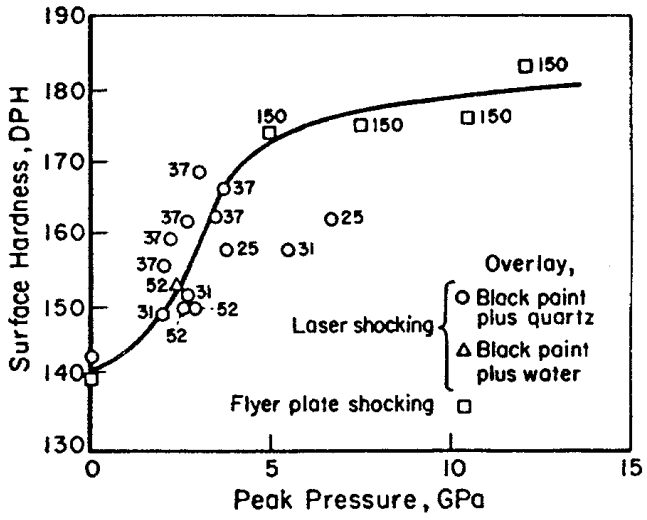

a. 2024-T351

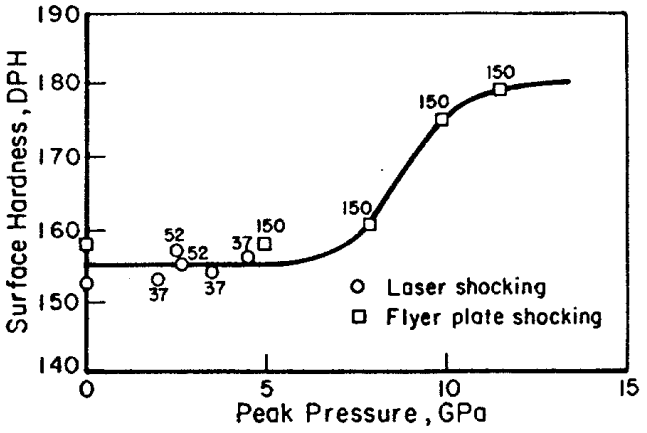

b. 2024-T851

Fig. 2. Dependence of Surface Hardness of 2024 Aluminum on Shock Wave Peak Pressure Compared to Surface Hardness from Flyer Plate-Induced Shock Pressures Taken from Herring and Olson (14). The Pulse Length in nsec is Written by Each Data Point.

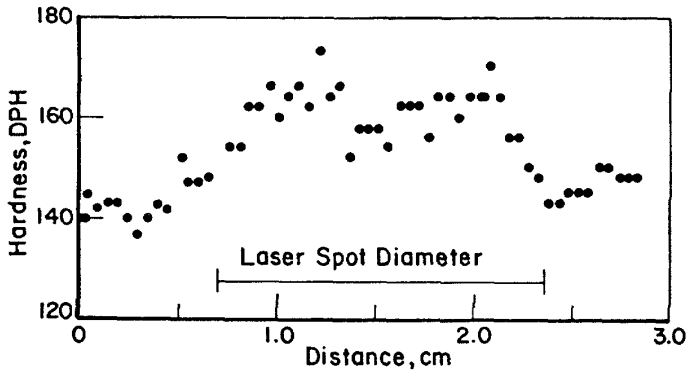

Fig. 3. Surface Hardness Profile Across a Laser Irradiated Spot on a 2024-T351 Disc. The Laser Pulse was 25 nsec Long at a Peak Pressure of 5.8 GPa with a Black Paint Plus Quartz Overlay.

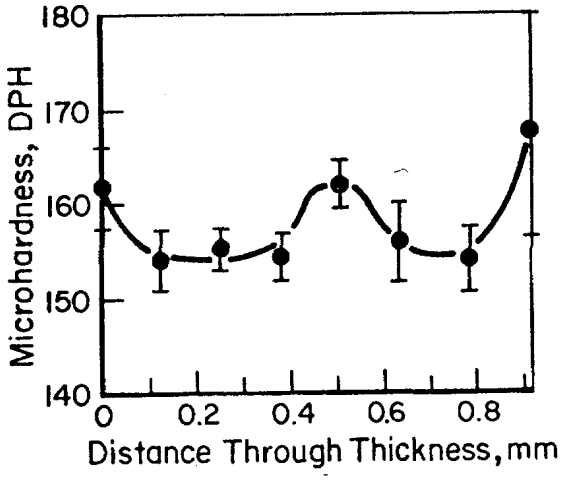

Fig. 4. Variation of Hardness Through the Specimen Thickness of 2024-T351 Shock on Both Surfaces Simultaneously. The Specimen was Shocked with Black Paint Plus Quartz Overlay a Pulse Length of 37 nsec, and a Peak Pressure on Either Side of 3.7 and 3.4 GPa.

7075 Aluminum Alloy. The 7075 alloy was studied less extensively than the 2024 alloy, The peak pressure range was similar, but the number of laser conditions were fewer than for 2024.

This was in part because the response of the 7075 alloy was less than that of the 2024. Neither of the 7075 heat treat conditions showed any shock hardening over the pressure range studied, up to 4.5 GPa for 7075-T651 and up to 2.8 GPa for 7075-T73.

The 7075-T651 alloy showed no discernable change in yield or tensile strength after laser shocking to 4.5 GPa*. An earlier result of laser shocking 7075-T651 to 3.0 GPa suggested a possible slight decrease in tensile strength after laser shocking. Jacobs reported that shocking 7075-T651 at 20.4 GPa with a driver plate increased the yield strength by 14 percent and the ultimate strength by 5 percent in one case and decreased both by 6 percent and 12 percent, respectively, in another case, which he attributed to improper cooling after shocking (2).

The tensile strength of the overaged, 7075-T73 condition, increased after laser shocking as expected from a previous study. The yield and tensile strengths increased by 15 to 10 percent respectively after shocking at 2.8 GPa with no loss in ductility. Larger increases of 29 and 14 percent increases in the yield and ultimate strengths respectively were reported by Fairand, et al for 7075-T73 aged to a lower initial yield strength** (23). In contrast, Jacobs reported that after shocking at 20.4 GPa the yield strength and ultimate strength of 7075-T73 were increased by only 11% and 3%, respectively. Thus it appears that most of the shock hardening of 7075-T73 is reached at relatively low peak shock pressures and amounts to about a 15% to 30% increase above the unshocked strength. There was no decrease in elongation in this study, but the other investigations reported decreases in elongation after laser shocking (10,19). Also, in this investigation, the yield strength of the shocked 7075-T73 specimen is higher than the ultimate tensile strength of the unshocked specimens (17). Even with this substantial increase in tensile strength the surface hardening was very small, an interesting exception to correlations between hardness and flow stress, suggested by others, and which was found to be consistent with laser shocking of weld zones in 6061 aluminum (24,25,19).

It is interesting to compare the change in tensile flow stress of 7075-T73 after shocking compared to tensile strain hardening. The total true transient strain after shocking, ε_T, can be calculated using the relation by Dieter

$$\varepsilon_T = \frac{4}{3} \ln \frac{v}{v_o} \quad , \qquad (1)$$

---

*The unshocked tensile properties of the 7075-T651 were 532 MPa 0.2 percent offset yield strength and 581 MPa ultimate strength. The same properties of the 7075-T73 were 408 MPa 0.2 percent offset yield strength and 476 MPa ultimate strength (17).

**The unshocked tensile properties were 345 MPa 0.2 percent offset yield strength and 514 MPa ultimate strength (23).

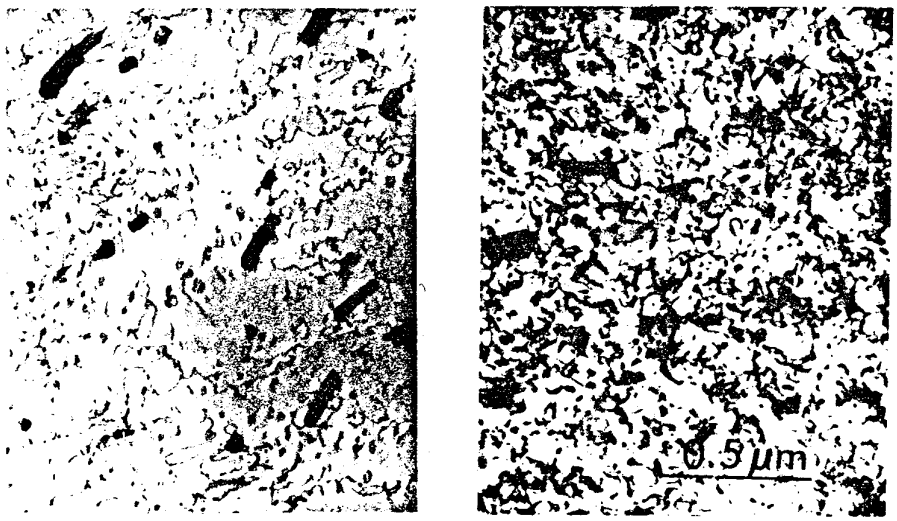

a. 2024-T351 Unshocked.

b. 2024-T351, Shocked.

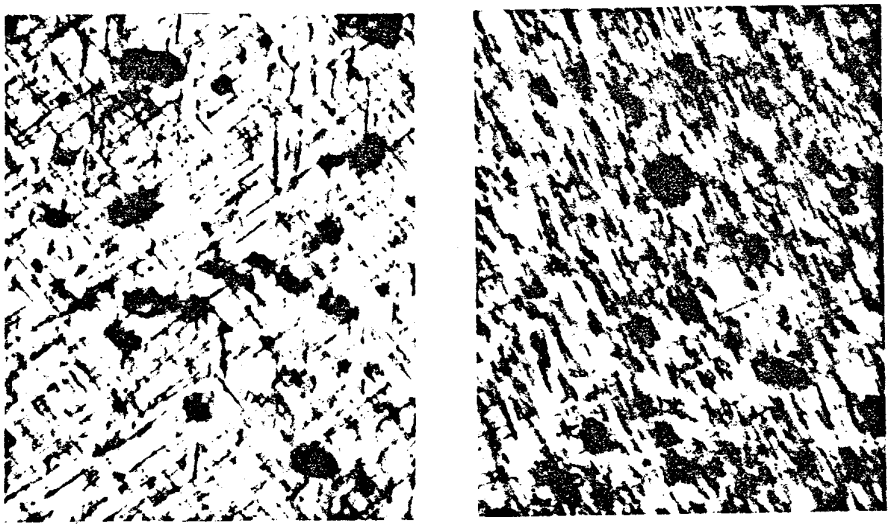

c. 2024-T851, Unshocked.

d. 2024-T851, Shocked.

Fig. 5. Transmission Electron Micrographs of the 2024 Alloy Before and After Laser Shocking. The 0.3 cm Thick Discs were Shocked on Both Sides Simultaneously Using Black Paint Plus Quartz Overlay. The 2024-T351 was Shocked with a Pulse Length of 25 nsec and Peak Pressures of 4.4 and 5.2 GPa on Either Side. The 2024-T851 was Shocked with a Pulse Length of 25 nsec and Peak Pressures of 3.2 and 3.4 GPa on Either Side.

where v is the volume of the alloy at the peak shock pressure, 2.6 GPa, and v_o is the volume at ambient pressure (26). The calculation gives ε_T = 0.041, which is somewhat higher than the actual strain because the maximum surface pressure was used for the calculation and the average in-material pressure would be lower (Figure 1). The flow stress of the shocked material is 479 MPa (0.2 percent offset yield strength). Compared to this the ultimate tensile strength of the unshocked material, corresponding to the flow stress at 0.06 tensile strain, is 476 MPa. Thus, the shock-induced strain hardens the material equivalent to or more than a higher tensile strain. A similar effect was observed in 2024-T3 when comparing ε_T to strain introduced by cold rolling (16).

The reason for the higher proportional strengthening of 7075-T73 compared to 7075-T651 is not related to the strain hardening rate as it might have been in the 2024 aluminum since it is similar for both conditions. However, the overall strength level before laser shocking was much lower for 7075-T73 than for 7075-T651 and what laser shocking did was to raise the flow stress over the entire tensile stress-stain curve. This strengthening is evidently due to the higher shock induced dislocation density of the 7075-T73 compared to the 2024 and 7075-T651. The microstructures for the 7075 alloy before and after shocking are shown in Figure 6. It is notable that the dislocation substructure in 7075-T73 after laser shocking is much denser (Figure 6d) than in any of the other materials (Figures 5b and d and 6b) even though the peak pressure was not larger than for the others. Also bands of dislocations hinted at in the shocked 7075-T6 (Figure 6b) are well developed in the shocked 7075-T73 (Figure 6d). Jacobs did not observe bands in 7075-T6 after shocking at 20.4 GPa either; he reported only a much finer substructure compared to that shown in Figure 6b.

EFFECT OF LASER SHOCKING ON FATIGUE PROPERTIES

Since a laser induced stress wave produces the highest inelastic strain in the near surface region of aluminum alloys, similar in effect to shot peening, it was of interest to investigate the effect of laser shocking on fatigue properties. The fatigue properties investigated in the initial experiments discussed below were fretting fatigue of a fastener joint configuration and fatigue crack propagation. The alloy selected was 7075-T6 aluminum plate, 0.48 cm thick.

Specimen Preparation

The specimen geometry for the fretting fatigue specimen is shown in Figure 7. The crack propagation specimens were large rectangular plates 61 x 10.8 x 0.47 cm in size. The crack starters were two holes drilled along the centerline of the specimen 20.3 cm apart evenly spaced from the middle of the length of the specimen. The specimens were first machined without drilling the fastener holes in the fretting fatigue specimen or the two central holes in the crack growth specimens. After machining, two fastened joint specimens and one crack propagation specimen were laser shocked with a 1.3 cm diameter spot size centered on the fastener holes as indicated in

Figure 7 and the crack growth holes. The specimens were shocked on both sides simultaneously using the split beam with a black paint and fused quartz overlay and a laser beam pulse length of 23 nsec and power density of about 2.7 x 10^9 W/m^2. This corresponds to a peak pressure of about 5.7 GPa. After laser shocking, holes 0.48 cm in diameter were drilled in the laser shocked specimens with the hole centerline aligned with the center of the 1.27 cm diameter laser shocked region. Likewise, identical holes were drilled in the unshocked specimens at the same locations.

The load transfer fretting fatigue specimens were designed to give approximately a 30 percent stress differential between the pad and the strip. The resulting difference in the elastic extension of the two pieces created relative movement between the two pieces, leading to rubbing contact and ultimately to fretting fatigue failure. The rubbing contact was forced into the laser shocked region around the fastener hole by grinding the surrounding unshocked region away slightly. The fretting fatigue specimens were then assembled and the fastener* was inserted in the fastener hole, joining the pad and the strip, Figure 7.

Fretting Fatigue

A total of two shocked and two unshocked fastened joint specimens were tested in a Krouse fatigue machine. At first the maximum stress loading was set at 96.5 MPa in order to evaluate the fretting mode of failure, i.e., high cycle failure. The stress ratio for these tests was 0.1. The results of the fretting fatigue tests are shown in Table 1. The average life of the unshocked specimens was less than 500,000 cycles at 96.5 MPa and about half of that at 116 MPa maximum stress amplitude. The specimens which were laser shocked in the region of the fastener hole had dramatically longer lives. One shocked specimen had over 48 million cycles accumulated at 96.5 and 106 MPa maximum stress amplitude, before raising the stress to 116 MPa caused failure after 250,000 cycles. The second specimen accumulated 15 million cycles at 96.5 MPa before failing when the maximum stress amplitude was increased to 116 MPa.

After failure the fracture surfaces of the specimens with and without laser shocking were examined by scanning electron microscopy. A common feature for both the shocked and unshocked specimens was the existence of a layer of material at the fretted surface about 80 to 150 μm thick. A representative area is shown in Figure 8 from an unshocked specimen. This layer is probably a severely worked region resulting from the contact shear stresses caused by the relative movement between the rubbing surfaces of the pad and the strip. The work hardened layers appear to have about the same thickness in the shocked and unshocked specimens after fatigue, but there is an apparent difference in the appearance of the fracture surface of this layer. In the unshocked specimens it appears to be relatively smooth and featureless compared to the rest of the fracture surface (Figure 8), but in the shocked specimens this layer has a noticeably 'rougher' surface (A in Figure l0a).

---

*The fastener was a straight shank alloy steel aerospace quality fastener with a torque-off collar.

Table 1. Influence of Laser Shocking on Fretting Faitugue Failure of Fastened Joints in 7075-T6 Aluminum

Specimen	Condition	Maximum[(a)] Stress, MPa	Total Cycles at Stress	Total Fatigue Life, Cycles
1	Unshocked	96.5		501,000
2	Unshocked	96.5		408,000
3	Unshocked	116		236,000
4	Laser Shocked	96.5	32,090,000	
		106	16,300,000	
		116	259,800	48,649,800
5	Laser shocked	96.5	15,076,000	
		116	384,000	15,460,000

(a) Stress Ratio = 0.1.

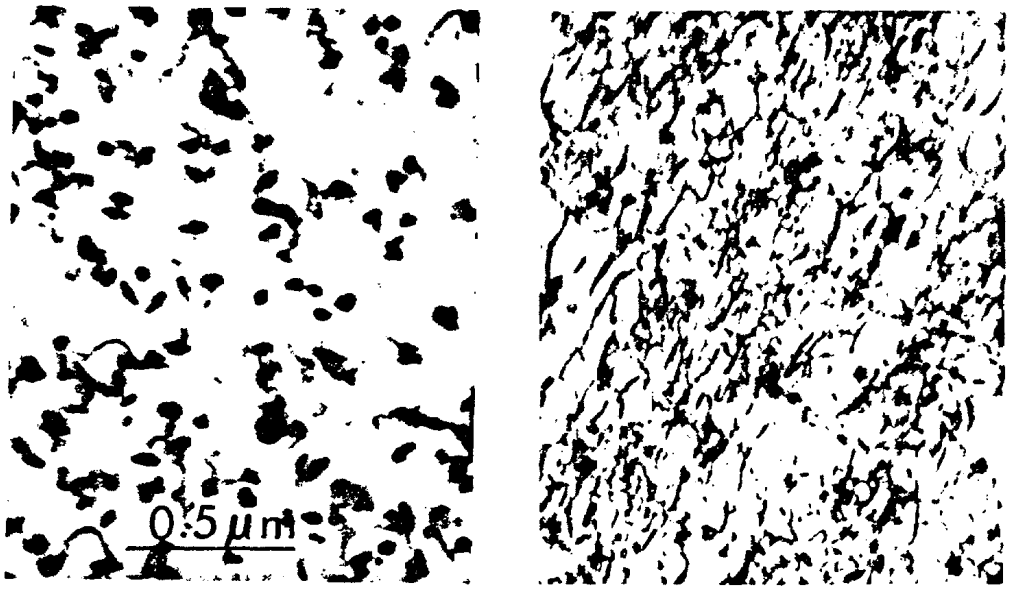

a. 7075-T65, Unshocked. b. 7075-T65, Shocked.

c. 7075-T73, Unshocked. d. 7075-T73, Shocked.

Fig. 6. Electron Transmission Micrographs of the 7075 Alloy Before and After Laser Shocking. The Specimens were the Same as the 2024 Alloy (Figure 5). Both Alloys were Shocked with a Laser Pulse Length of 52 nsec and Peak Pressures on Either Side of 3.3 and 3.5 GPa.

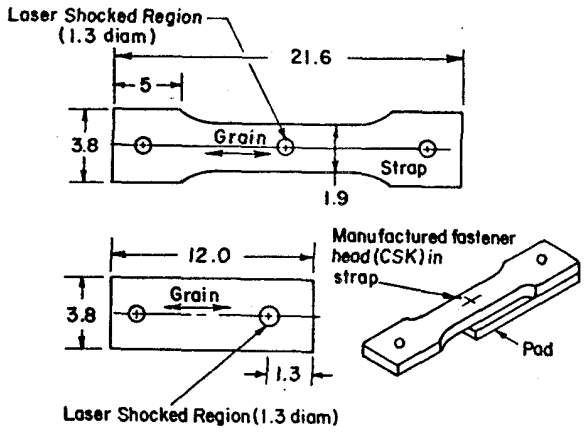

Fig. 7. Geometry of the Fretting Faitgue Specimen. The Dimensions are Given in Centimeters.

The vertical striations in Figure 8 are discontinuities in the fracture surface at grain boundaries. The grains are flattened in the plane of rolling, causing the grain boundaries to be aligned parallel to the specimen surface in this view.

It appears to be the work hardened surface layer which spalls off during the test and gives the pitted appearance to the contact region around the fastener hole on both shocked and unshocked specimens. A representative region of the rubbed surface is shown in Figure 9 where a specimen has been tilted at an angle to the viewing direction. The solid lines at the edges of the micrograph delineate the corner between the rubbing surface (lower half of the figure) and the fracture surface (upper half of the figure). There was extensive pitting on the rubbed surface in the lower part of the micrograph. Cracks between the work hardened surface layer and the underlying material are evident at the fracture surface and at the bottom of pitted regions (A in Figure 9). In this unshocked specimen, the fracture appears to have initiated at the bottom of a surface pit on the rubbed surface (0 in Figure 9).

There were no discernable inclusions or other features which could be specifically identified at the crack initiation site of the unshocked specimens. It appears that the material becomes so severely deformed in the rubbing contact regions that the material eventually separates locally after reaching some critical accumulated inelastic strain. Cracking might be encouraged in pitted areas by local stress concentrations at the base of surface ledges when these act as obstacles to sliding between the two surfaces.

In both shocked specimens the fracture origin was associated with a rounded or sphere-like ‘tab’ of material at the rubbing contact surface located at the edge of the contact area. This is shown at 0 in Figure 10a. In Figure 10a the specimen is tilted like that in Figure 9. The solid lines delineate the edge of the fracture surface. The rubbed region is severely pitted or scored. The

work hardened surface layer is not so easily seen here as in Figure 8, but part of it is pointed out at A. No inclusions or other distinguishable microstructural features could be discerned at the crack initiation site, Figure 10b.

Although there is a striking improvement in fretting fatigue life after laser shocking, no conclusions about the strengthening mechanisms can be reached on the basis of these limited data. Fretting fatigue is a complex failure process which is not sufficiently well understood in the absence of laser shocking to attempt to identify the particular mechanism by which laser shocking has extended the fretting fatigue life in these experiments (27). However, several considerations influencing this behavior can be pointed out based on the effects of laser shocking on these aluminum alloys. One of the effects described earlier is the shock hardening of the surface and near-surface region. Another effect is that laser shocking appears to create a compressive residual stress in the surface. Several limited measurements of laser shocked 7075-T651 and 2024-T351 using x-rays showed the residual stresses to be small, less than ten thousand psi, and compressive in sign. The residual compressive surface stress will certainly act to inhibit the opening of surface cracks during fretting and retard crack propagation. This will lengthen the crack initiation stages and propagation and increase fatigue life. The effect of the shock hardening of the surface layer is not clear. Another method for introducing compressive residual surface stress and a work hardened surface layer, in the region around the fastener hole, i.e., shot peening, is not as effective in increasing fretting fatigue life as laser shocking though the magnitude of the residual stress appears to be greater after shot peening.

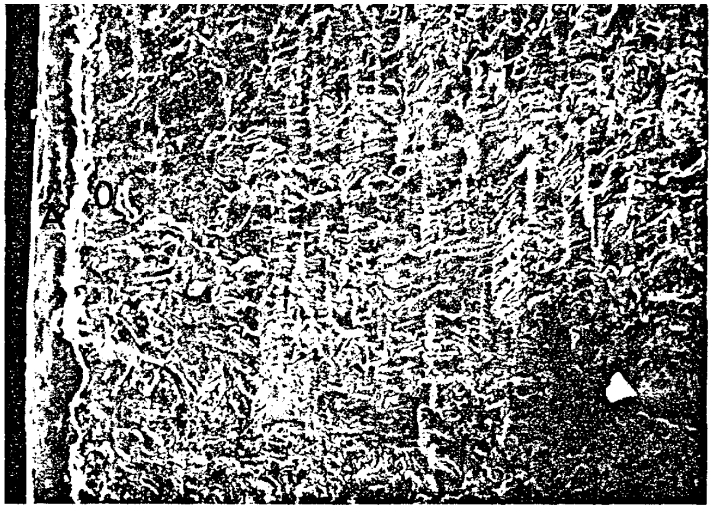

100X

Fig. 8. Fracture Surface of Unshocked Specimen No. 2 After Fretting Fatigue Failure. The Strain Hardened Surface Layer is Indicated at A and the Region of the Fracture Origin by O.

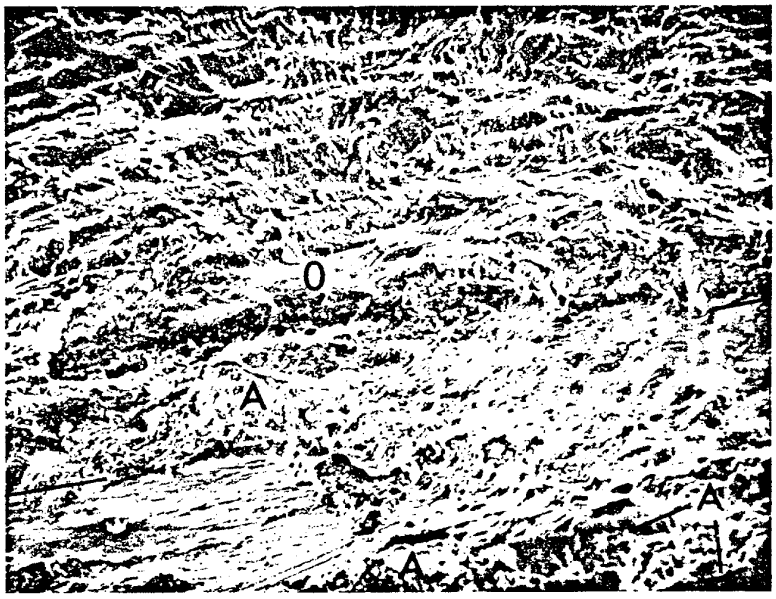

100X

Fig. 9. The Fracture Surface (Upper Half) and Rubbing Contact Surface (Lower Half) of Unshocked Specimen No. 1 Tilted to an Angle to the Viewing Direction. Cracks are Marked at A and the Fracture Origin at O.

At this point, several ways to rationalize this ambiguity come to mind. It may be that what is necessary is an optimum balance between the residual surface stress and the degree of surface cold work. This is because increasing cold work tends to decrease the ductility of a metal and will make it susceptible to cracking at a lower accumulation of fatigue strain. This effect could offset the beneficial effects of higher surface hardness and residual compressive stresses. This explanation requires that modest residual compressive stresses remain effective when coupled with the small plastic surface strains caused by the shock hardening. Another consideration is that there may be differences in the type of hardening dislocation microstructure created by laser shocking and shot peening, differences which are important in increasing the fretting fatigue life after laser shocking. The difference in the appearance of the fracture surface of the work hardened surface layer might relate to a significant difference in the work hardening and fracture behavior of this layer after laser shocking. If this is so, it is possible that this might be associated with the longer fretting fatigue life, i.e., a longer time to develop the appropriate microstructural conditions for crack initiation. Lastly, the surface rubbing conditions might be so severe that the crack initiation stage is not extended very much by laser shocking. The specific microstructural effects of the shock hardening are soon wiped out in the surface layer and crack initiation proceeds as without laser shocking. However, as will be seen in the next section, fatigue crack propagation appears to be slowed dramatically in the laser shocked zone. It may be that a prolonged crack propagation

stage is an importance factor in increasing the fretting fatigue life.

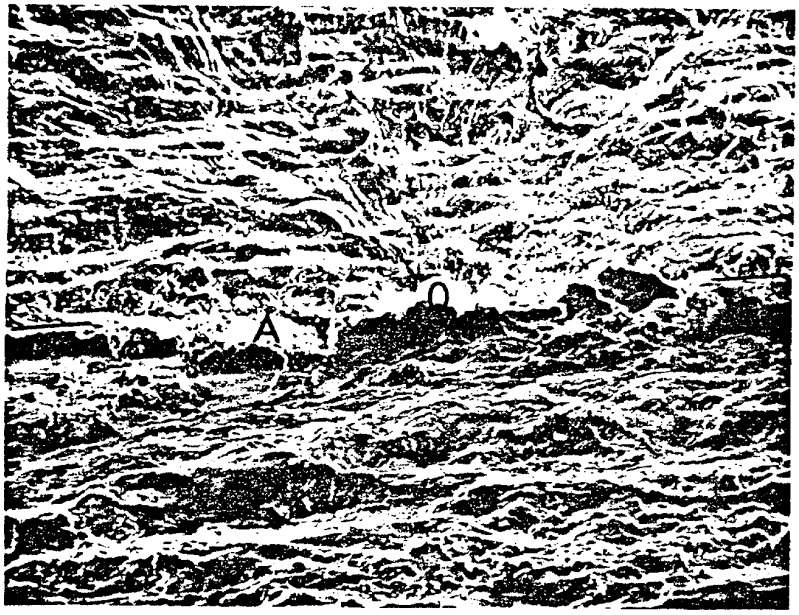

100X

a. The fracture surface (upper half) and rubbing contact surface (lower half) of shocked specimen No. 5. Part of the surface layer is marked at A and the crack initiation site is marked at 0.

500X

b. The crack initiation site in (a) above.

Fig. 10. The Rubbing Contact and Fracture Surfaces in Shocked Specimen No. 5.

Fatigue Crack Propagation

The crack growth specimens were tested in a Krouse fatigue machine at an 82.7 MPa gross section stress. A crack initiation site was introduced in each of the holes prior to testing by notching the sides of the holes with a saw. The unshocked specimen experienced full width fatigue failure at 430,000 cycles from one hole. The other hole had a crack approximately 2 cm long attached to it at failure. The shocked specimen never did fail at the laser shocked holes. Repeated failure of the specimen grips necessitated terminating the experiment after 2,300,000 cycles. Maximum crack growth at that time was 0.08 cm.

Instead of a single crack propagating to failure as observed in the unshocked specimens (Figure 11a), several small cracks were seen to be emanating from the notched hole of the shocked specimen (Figure 11b). During the fatigue test the individual cracks did not propagate uniformly. Instead, one or the other of the cracks propagated ahead of the rest and then stopped while another began to propagate and moved out ahead. Because of this, the crack growth rate could only be approximated and it was decided to measure the length of the longest crack each time to obtain dA/dN for the laser shocked condition. With this qualification, an approximate comparison of the shocked and unshocked fatigue failure levels can be made using the calculated crack growth per cycle, dA/dN. Based on a comparison at 430,000 cycles, dA/dN for the unshocked specimen was 3×10^{-7} m per cycle and for the shocked specimen it was 2×10^{-10} m per cycle, which is an improvement in dA/dN of about 1500 times. The rate of crack growth in the shocked specimen was still nearly linear at 2,300,000 cycles.

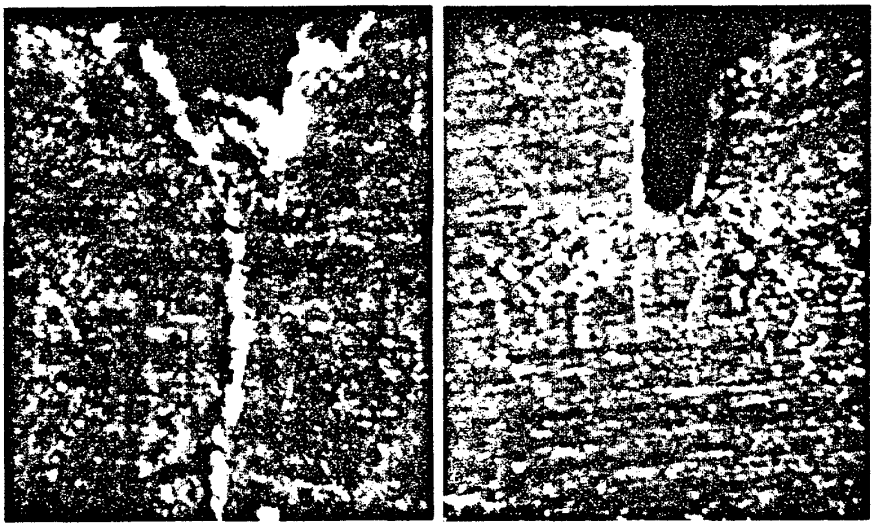

a. Unshocked, 430,000 cycles. b. Shocked, 2,300,000 cycles.

Fig. 11. The Effect of Laser Shocking on the Appearance of Fatigue Cracks at the Starter Notch in the Crack Propagation Specimens.

The reason for this dramatic decrease in crack propagation rate in the laser shocked region is not clear. If surface residual compressive stresses were the cause, then one would expect shot peening to have a much larger effect on crack propagation rate because of the larger residual stresses. The surface opening of the cracks appear to be much tighter on the laser shocked surface compared to the unshocked surface. Alternatively, it may be that deeper hardening effects of the laser shocking process compared to shot peening provides a significant retarding interaction with the propagating crack.

CONCLUDING DISCUSSION

Laser shock-induced hardening of aluminum alloys is feasible in the underaged 2024-T351 and overaged 7075-T73 alloys. The yield strength is increased in both alloys but the ultimate strength is increased in 7075-T73 only. This is similar to the response of the welded 5086 and 6061 alloys reported earlier in which the yield strength was increased substantially and the ultimate strength was increased only a modest amount after laser shocking. There is further potential for hardening the 2024-T351 by increasing the peak pressures (increasing power densities), whereas the 7075-T73 appears to be shock hardened to most of its potential at the present levels of peak pressures (2 to 5 GPa) and further increase in shock pressure may not provide much more strengthening.

It is interesting to review the response of the 7075-T6 alloy to laser shocking. The surface hardness and tensile strength showed no increase after laser shocking to peak pressures of 3.5 GPa in this study and 3.7 GPa in the study of Fairand, et al (23). However, this material showed a dramatic increase in fretting fatigue life and decrease in crack propagation rate in the laser shocked zone. However, the relative importance of laser shocking on the crack initiation stage and crack propagation stages during fretting fatigue is not known. The reasons for these effects are not known, but they must result from the particular combination of residual surface compressive stresses and in-depth distribution and amount of inelastic strain produced by the shock wave. There was clear transmission microscopy evidence of laser shock induced increases in dislocation density. These effects are the only ones identified so far by which laser shocking modified the state of the material, but their relative importance cannot be determined here. Although it is reasonably certain that the residual surface stresses are compressive for the shocking conditions used here, the magnitude of these stresses is not, although they appear to be small.

ACKNOWLEDGMENTS

The authors acknowledge the support of the National Aeronautics and Space Administration under Contract No. NASI-14047 for part of the research reported in this paper. The close collaboration of Stephan C. Ford in the investigation of fretting fatigue and crack propagation is gratefully acknowledged. Also we wish to acknowledge the help of Bernard Campbell for assisting with the laser experiments and Marjorie Cantin for assisting with the materials evaluation.

REFERENCES

(1) D. Voss, and T.M.F. Ronald, "Microstructure and Mechanical Property Modification of Plastic Wave TMT 7075 Aluminum", paper presented at AIME Spring Meeting, 1973.

(2) A. J. Jacobs, "The Mechanism of Stress Corrosion Cracking in 7075 Aluminum", Proc. Conf. on Fundamental Aspects of Stress Corrosion Cracking; Ed. R. W. Staehle, et al., National Association of Corrosion Engineers, 1969, p. 530.

(3) R. N.. Orava, "Explosive Thermomechanical Processing", Kramer, I. R., et al., ed., Final Report No. AMMRC CR 66-05/31(f), Martin-Marietta Corp., 1972.

(4) A. H. Clauer, B. A.. Wilcox, and B. D. Trott, "Thermomechanical Processing of 7075 Aluminum Alloy Plate Using Plastic Shock Wave", Research on Metallurgical Synthesis, AFML-TR-72-238, Part II, Battelle Columbus Laboratories, 1974, p. 158.

(5) C. A. Askar yan and E. M. Moroz, "Pressure on Evaporation of Matter in a Radiation Beam", JETP Lett., Vol. 16, 1963, p. 1638.

(6) R. M. White, J. Appl. Phys., Vol. 34, 1963, p. 2123.

(7) N. C. Anderholm, "Laser Generated Stress Waves", AppI. Phys. Lett., Vol. 16, 1970, p. 113.

(8) J. A. Fox, Appl. Phys., Lett., Vol. 24, 1974, p. 461.

(9) L. C. Yang, "Stress Waves Generated in Thin Metallic Films by a Q-Switched Ruby Laser", J. Appl. Phys., Vol. 45, No. 6, 1974, p. 2601.

(10) B. P. Fairand, A. H. Clauer, R. G. Jung, and B. A. Wilcox, "Quantitative Assessment of Laser-Induced Stress Waves Generated at Confined Surfaces", Appl. Phys. Lett., Vol. 25, 1974, p. 431.

(11) B. P. Fairand, and A. H. Clauer, "Effect of Water and Paint Coatings on the Magnitude of Laser-Generated Shocks", Opt. Comm., Vol. 18, 1976, p. 448.

(12) B. P. Fairand, and A. H. Clauer, "Laser Generation of High Amplitude Stress Waves in Materials", J. Appl. Phys., accepted for publication in Spring of 1979.

(13) A. H. Clauer, B. P. Fairand, and B. A. Wilcox, "Pulsed Laser Induced Deformation in a Fe-3 Wt.% Si Alloy", Met. Trans. A, Vol. 8A, 1977, p. 119.

(14) R. B. Herring, and G. B. Olson, "The Effect of Aging Time on Spallation of 2024-T6 Aluminum", AMMRC TR71-61, Army Materials and Mechanics Research Center, December, 1971.

(15) A. S. Appleton, and J. S. Waddington, "The Importance of Shock Wave Profile in Explosive Loading Experiments", Act. Met., Vol. 12, 1964, p. 956.

(16) S. La Rouche and D. E. Mikkola, "Shock Hardening Behavior of Cu-8.7 Ge at Very Short Pulse Durations", Vol. 12, No. 6, 1978, p. 543.

(17) A. H. Clauer, B. P. Fairand and J. E. Slater, "Laser Shocking of 2024 and 7075 Aluminum Alloys", NASA CR-145132, Battelle Columbus Laboratories, 1977.

(18) H. Otto, "Shock Hardening of Aluminum Alloys", High Strain Rate Behavior of Metals Session, WESTC Conference, March, 1979, Los Angeles.

(19) A. H. Clauer, B. P. Fairand, and B. A. Wilcox, "Laser Shock Hardening of Weld Zones in Aluminum Alloys Met. Trans. A, Vol. 8A, 1977, p. 187.

(20) D. J. Antrobus, and C. N. Reid, "Precipitation Hardening of Shock Loaded Aluminum Alloys", Final Report for Ministry of Defense, University of Birmingham, Great Britain, March, 1972.

(21) J. S. Waddington, Ph.D. Thesis, University of Liverpool, 1964.

(22) M. F. Rose, and T. L. Berger, "Shock Deformation of Polycrystalline Aluminum", Phil. Mag., Vol. 17, 1968, p.1121.

(23) B. P. Fairand, B. A. Wilcox, W. J. Gallagher, and D. N. Williams, J.Appl. Phys., Vol. 43, No. 9, 1972, p. 3893.

(24) I. D. Tabor, The Hardness of Metals, Clarendon Press (Oxford), 1961.

(25) J. R. Cahoon, W. H. Broughton, and A. R. Kutzak, "The Determination of Yield Strength Form Hardness Measurements", Met. Trans., Vol. 2, 1971, p. 1979.

(26) G. E. Dieter; Metallurgical Effects of High-Intensity Shock Waves in Metals, Response of Metals to High Velocity Deformation, P. G. Shewman, and V. F. Zackay, ed., Interscience, 1960, p. 409.

(27) Control of Fretting Fatigue, National Materials Advisory Board, NMAB-333, 1977.